PHYSICAL REVIEW D VOLUME 27, NUMBER 7 1 APRIL 1983

Radial spectra and hadronic decay widths of light and heavy mesons

E. van Beveren, G. Rupp, T. A. Rijken, and C. Dullemond
Institute for Theoretical Physics, University of Nijmegen, Nijmegen, The Netherlands
(Received 23 March 1982)

A potential model for mesons is presented, which combines quark confinement and strong decay in a realistic approach. The multichannel Schrödinger formalism is employed to describe a system of one or more permanently closed quark-antiquark channels in interaction with several two-meson channels. For the potential in the $q\bar{q}$ channels a harmonic oscillator with constant frequency is taken. As for the meson channels only Okubo-Zweig-Iizuka-rule-allowed decays into two mesons of the pseudoscalar or vector type are considered. Final-state interactions between these mesons are not yet taken into account. The communication between confined and free channels is supposed to take place via the $^3P_0$ mechanism, for which a locally approximated transition potential is derived. In order to obtain an analytic solution for the S matrix, the transition potential is treated by using a multi-δ-shell method. Kinematically relativistic corrections and color splitting allow a fairly successful treatment of pseudoscalar as well as vector mesons for all quark flavors. The results are confronted with the data and discussed.

I. INTRODUCTION

This paper is the second of a series of papers on the spectra of mesons and baryons based on a model, which we have proposed recently.[1,2] In Ref. 2 preliminary results of the model for charmonium and b-quarkonium systems are given. In this paper we achieve a universal description of the light mesons π, η, ρ, ϕ,... as well; we extend our model to include a treatment of both the heavy and light quarks.

It is a rather well known fact that the level spacings of the first few radial excitations of the ψ and the Υ systems are remarkably similar. We note that this kind of universality (i.e., level spacing independent of the constituent quark mass) extends to, for example, the ρ and ϕ systems as well, if one assigns the first radial ρ excitation to the state at 1250 MeV (Ref. 3), the second one to the state at 1600 MeV (Ref. 4), and if the recently reported ϕ resonances at 1650 MeV (Ref. 5) and 1900 MeV (Ref. 6) may be identified with the first and second radial ϕ excitations, respectively. This universality is one of the important features of our model and distinguishes it from other models.[7-10]

Many quark models have already been proposed in the past. Their basic ingredient is the principle of confinement, which is taken into account by means of mechanisms (boundary conditions,[7] rising potentials[8,9]), which permanently bind the quarks to a hadron, thus describing hadrons in first instance as being stable systems even with respect to strong decays. Very often the effects of strong decay are underestimated. Exceptions are Refs. 10 and 2. Both Refs. 10 and 2 note substantial influence on the spectra and wave functions, but differ qualitatively.

As far as the binding mechanism is concerned our approach is comparable to what many authors have proposed, but considering hadrons as stable systems provides in our opinion a too simplified and, as we have shown explicitly in Ref. 2, an incorrect picture.

Let us illustrate this last remark by considering, for example, the state $\psi(4030)$. We might distinguish several components: in one component the charmed quark and the charmed antiquark are kept together by the confining force; the other components contain mesons with open charm (such as D, $\bar{D}$, F, $\bar{F}$, etc.). The coupling between the $c\bar{c}$ and open-charm components is provided by the creation or annihilation of a light-quark and antiquark pair.

In this investigation we limit ourselves to the creation or annihilation of only one $q\bar{q}$ pair, which means that we do not consider three- (or more) meson channels. This is reasonable since multimeson channels have a smaller effective coupling to the decaying meson and have therefore less influence on the binding forces between the quark and the antiquark in a meson.

A basic ingredient of our model, which has been described already in Ref. 2, is that the coupling between the quark-antiquark channels and the two-meson channels is accounted for properly by employing the coupled-channel Schrödinger formalism. The use of the Schrödinger equation guarantees (i) a unitary scattering matrix, (ii) proper threshold behavior of amplitudes, (iii) good analyticity proper-

ties, and (iv) Wigner causality.

A nonrelativistic Schrödinger model examined in Ref. 11 serves as a starting point. In Ref. 11 we studied the behavior of Regge poles in the complex angular momentum plane of a two-component scattering model. One of the channels in this model is permanently closed by means of a harmonic-oscillator potential representing the $c\bar{c}$ component. In the other channel(s) the scattering takes place, which represents the open-charm component(s). The transition potential in Ref. 11 was constructed by using only one spherical δ shell. In retrospect this was not a bad approximation of the more realistic $^3P_0$ transition potential which we use in this paper (see below). For small coupling the resonance positions are near to the bound-state positions of the harmonic oscillator in the absence of coupling. For larger coupling the original harmonic-oscillator spectrum is deformed drastically. In Ref. 2, we have shown that particularly the bound states, which lie below the threshold of the scattering channel or below the threshold of the most dominant scattering channel(s), if there are more of them, are shifted to much lower energies, especially the ground state. As we have shown in Ref. 2 the spectra of charmonium and b-quarkonium indeed exhibit this feature.

In extending the model as presented in Ref. 2 to the light-quark systems such as π, ρ,..., we apply kinematic relativistic corrections to the Schrödinger equation. These corrections are derived by means of a standard reduction and transformation[12] of a system of coupled-channel two-body Bethe-Salpeter equations to a coupled-channel Schrödinger equation in configuration space. (Notice in this context that we use constituent quarks, which are quite heavy in contrast to current quarks.) As in Ref. 2 we use a flavor-dependent harmonic-oscillator potential in the quark-antiquark channel to describe the confining forces.

In order to implement universality the confining potential is taken to be proportional to the constituent quark mass, which leads to a common basic frequency ω for all quark-antiquark systems. We comment briefly on this point in the next section. A second reason for taking a harmonic potential is that it is solvable analytically. This is important for the obtainment of an analytic approximation (see Appendix A) of the S matrix, which facilitates enormously the tracing of the bound-state and resonance poles in the complex energy plane. We derive the transition potential between the quark-antiquark channels and the two-meson channels using the $^3P_0$ model for the meson decays.[13,14] The latter model has been applied successfully to meson decay by several authors.[15,16]

TABLE I. Masses of $J^{PC}=1^{--}$ meson resonances in GeV. We use the spectroscopic notation $n\,^{2S+1}L_J$, where n is the number of radial nodes + 1, S is the total $q\bar{q}$ spin (0 or 1), L is the orbital angular momentum of the $q\bar{q}$ system, and J is the total angular momentum of the state.

Level	$1\,^3S_1$	$2\,^3S_1$	$3\,^3S_1$	$4\,^3S_1$	$1\,^3D_1$	$2\,^3D_1$
ρ	0.770	1.25	1.60			
ϕ	1.020	1.65	1.90			
ψ	3.095	3.684	4.03	4.414	3.772	4.16
Υ	9.435	9.993	10.32	10.59		

To maintain the universality of the spectra it is necessary to have a dependence of the transition potential parameters on the quark masses. This dependence can be explained in a natural way as will be discussed later.

The impact of the two-meson channels on the spectra of the mesons is very substantial (see also Ref. 2). In our model it turns the harmonic-oscillator spectra into realistic ones.

This paper is organized as follows: In Sec. II we discuss the data on which the ideas underlying our model are mainly based. In Secs. III and IV and Appendix A the Schrödinger equation is derived and solved for the S matrix. Sections V and VI are devoted to the transition potential. The results and their comparison with experiment are contained in Sec. VII, followed by the conclusions in Sec. VIII.

II. THE DATA

Before we explain the details of our model, we review some aspects of the present situation in hadron spectroscopy. We are particularly interested in the relative resonance positions of radial excitations.

A first observation is that the best experimental information on (radial) excitations is available for the negative-parity and negative-C-parity vector mesons and for the nucleon resonances. In Table I we give a classification of ground states and radial excitations of the $J^{PC}=1^{--}$ mesons.

The S states of Table I are depicted in Fig. 1, where some interesting regularities may be observed. The energy regions are totally different, but the en-

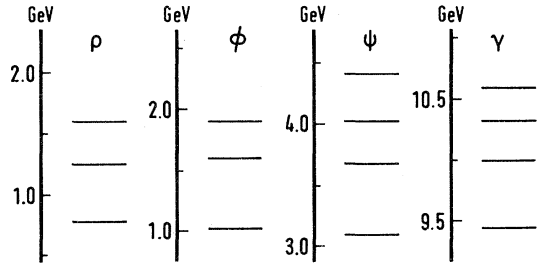

FIG. 1. Radial spectra of the ρ, ϕ, ψ, and Υ.

ergy splittings are very similar.

From Fig. 1 we draw the conclusion that a $q\bar{q}$ potential describing these spectra must have a flavor-mass dependence of the form

$$V(m,r)=V(\sqrt{m}\,r)\ , \tag{2.1}$$

where m is the flavor mass and r is the relative quark distance. Evidently a large class of potentials satisfies (2.1). As in Ref. 2 we use in this paper a harmonic-oscillator potential, which according to (2.1) must be proportional to the flavor mass (see also Ref. 1). It is known that the ψ and Υ spectra can be described by a flavor-independent potential as described in Ref. 10. However, this latter model would certainly not work for the ρ and ϕ resonances as classified in Table I. In the literature a flavor-independent potential is often motivated by referring to perturbative QCD. However, unperturbative QCD could very well lead to quite a different picture. For example, in a recent construction of Nielsen and Patkós,[17] confinement is described by a scalar field representing a color dielectric. Because of gauge invariance this scalar field couples to the quark kinetic energy. This leads to a picture of quarks moving in a potential which is linear in the quark mass. Then condition (2.1) results in the harmonic potential of this paper.

The assignments for the ρ and ϕ resonances are not established yet. If the ρ' (1250) (Ref. 3) is the $1\,^3D_1$ state rather than the $2\,^3S_1$ state, we may argue that for a slightly perturbed harmonic oscillator these resonances are in each other's neighborhood, in which case there should be a $2\,^3S_1$ ρ state in the energy region around 1250 MeV. This then implies

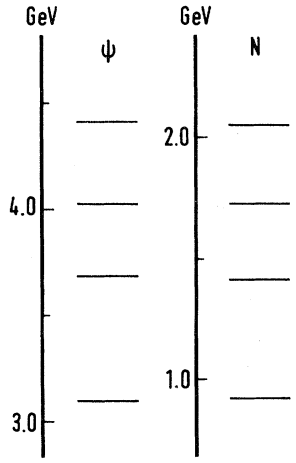

FIG. 2. Radial spectra of charmonium and the nucleon.

that the $\rho''(1600)$ could be the $3\,^3S_1$ ρ resonance. Similar arguments for the ϕ resonances and preliminary experimental results,[5] which indicate a ϕ state at 1650 Mev, lead to the classification shown in Table I.

In Fig. 2 we have compared the radial spectra of charmonium and nucleon resonances.[18,19] We see that the spectra are very similar. However, the spacings are different: the ratio of the mass differences of the first and third radial excitations of the ψ system [$\psi(4414)$-$\psi(3685)$] and of the nucleon $N(2050)$-$N(1410)$] equals 1.14. The mechanism of this ratio is not yet contained within our model. However, as we have seen in Ref. 2, the above spacing is related to the harmonic-oscillator frequency in the confined channel. So we conclude that it makes sense to investigate whether baryons may be treated similarly to mesons, but with a different oscillator frequency. This will be done in a subsequent paper.

III. THE MODEL

Consider a system of n quark-antiquark ($q\bar{q}$) channels in interaction with m two-meson (M_1M_2) channels:

$$a_i+b_i\rightarrow a_j+b_j\ . \tag{3.1}$$

Here each channel j consists of two particles (either $q\bar{q}$ or M_1M_2) a_j and b_j with momentum p_{a_j} and p_{b_j}.

The normalization of the one-particle states is

$$\langle a'\,|\,a\rangle=(2\pi)^3 2E_a(\vec{p}_a)\delta^3(\vec{p}_{a'}-\vec{p}_a)\delta_{s_{a'}s_a}\ , \tag{3.2}$$

where s_a and $s_{a'}$ are the third components of the particle spins. The S matrix and the M matrix are related by

$$\langle i\,|\,S\,|\,j\rangle=\langle i\,|\,j\rangle-i(2\pi)^4\delta^4(P_i-P_j)\langle i\,|\,M\,|\,j\rangle\ . \tag{3.3}$$

Here P_i and P_j are, respectively, the total final and initial four-momenta of the system. We introduce the relative momenta k_j by

$$p_{a_j}=w_aP_j+k_j,\quad P_{b_j}=w_bP_j-k_j \qquad (w_a+w_b=1)\ . \tag{3.4}$$

In our model we neglect the transition to negative-energy states and we also neglect the dependence of the interaction and the amplitudes

$M_{ij}=\langle i \mid M \mid j \rangle$ on the relative energies k_j^0. (Notice that we use constitutent quarks in our models, which are still fairly heavy, even in the case of the u and d quarks.) With these approximations the coupled-channel Bethe-Salpeter equation, which in first instance is apt to describe the coupled-channel system of our model, reduces to a Blankenbecler-Sugar-Logunov-Tavkhelidze-type equation[20]:

$$M_{ij}(\vec{k}_i,\vec{k}_j;\sqrt{s})=I_{ij}(\vec{k}_i,\vec{k}_j;\sqrt{s})+\sum_n \int d^3k_n I_{in}(\vec{k}_i,\vec{k}_n;\sqrt{s})g_n(\vec{k}_n;\sqrt{s})M_{nj}(\vec{k}_n,\vec{k}_j;\sqrt{s}) . \tag{3.5}$$

The Green's function $g_n(\vec{k}_n;\sqrt{s})$ is not unambiguous. In order to account for the relativistic velocities of the mesons in some channels (e.g., the pions in the case of the ρ system) we need a coupled-channel Schrödinger equation with relativistic kinematics. Therefore, we take[21,22]

$$g_n(\vec{k}_n;\sqrt{s_n})=\frac{\rho_n}{2\sqrt{s_n}}\frac{1}{\vec{k}^2(s)-\vec{k}_n^2(s_n)+i\epsilon} , \tag{3.6}$$

where

$$\sqrt{s_n}=E_{a_n}(\vec{k}_n)+E_{b_n}(\vec{k}_n)$$

and

$$\rho_n=[4E_{a_n}(\vec{k}_n)E_{b_n}(\vec{k}_n)]^{1/2} .$$

The transition to a relativistic Lippmann-Schwinger equation is performed via the definitions[20]

$$\langle a_i,b_i \mid T,V \mid a_j,b_j \rangle=\left[\frac{\rho_i}{2\mu_{ii}(E)}\right]^{1/2}\frac{\langle a_i,b_i \mid M,I \mid a_j,b_j \rangle}{2\sqrt{s}}\left[\frac{\rho_j}{2\mu_{jj}(E)}\right]^{1/2} , \tag{3.7}$$

where $s=s_i=s_j=E^2$, the total energy squared in the c.m. frame and where the elements of the $(n+m)\times(n+m)$ reduced mass matrix $\mu(E)$ are defined by

$$2\mu_{ij}(E)=(d\vec{k}_i^{\,2}/dE)\delta_{ij}=\frac{E_{a_i}E_{b_i}}{E_{a_i}+E_{b_i}}\delta_{ij} . \tag{3.8}$$

For convenience we define

$$\mu(E)=\begin{bmatrix} M_c(E) & 0 \\ 0 & M_f(E) \end{bmatrix} . \tag{3.9}$$

In (3.9) M_c is the $n\times n$ reduced mass matrix for the confined $q\bar{q}$ channels and M_f the $m\times m$ reduced mass matrix for the meson-meson channels. With (3.7)—(3.9) we get

$$T_{ij}(\vec{k}_i,\vec{k}_j)=V_{ij}(\vec{k}_i,\vec{k}_j)+\sum_n \int d^3k_n V_{in}(\vec{k}_i,\vec{k}_n)\frac{2\mu_{nn}(E_n)}{\vec{k}_i^{\,2}-\vec{k}_n^{\,2}+i\epsilon}T_{nj}(\vec{k}_n,\vec{k}_j) . \tag{3.10}$$

The corresponding coupled-channel relativistic Schrödinger equation reads

$$[-\Delta+2\mu(E)V-\vec{k}^2(E)]\psi=0 , \tag{3.11}$$

where ψ is the coupled-channel two-particle wave function.

The potential in (3.11) is spherically symmetric and might be represented by a symmetric $(n+m)\times(n+m)$ matrix

$$V=\begin{bmatrix} V_c & V_{\rm int} \\ V_{\rm int}^T & V_f \end{bmatrix} . \tag{3.12}$$

In (3.12) V_c is the potential in the confined channels

$$[V_c(r)]_{ij}=\delta_{ij}(\tfrac{1}{2}\mu_{ii}\omega^2r^2+C_i) , \tag{3.13}$$

where ω is the universal frequency, r is the relative distance in the $q\bar{q}$ system, and C_i is the ith diagonal element of a diagonal $n\times n$ constant matrix C. V_f is the diagonal threshold matrix. $[V_f]_{jj}=D_j$ is the sum of the rest masses of the bosons in the jth meson-meson channel.

The specific form of the off-diagonal term in (3.12) will be discussed in the next section.

Let $\phi(r)$ be a radial $(n+m)$-component wave function, then the set of radial Schrödinger equations to be solved is

$$\left[-\frac{d^2}{dr^2}+\frac{L(L+1)}{r^2}+2\mu(E)V(r)-\vec{k}^{\,2}(E)\right]\phi(r)=0\,, \quad (3.14)$$

where L is the orbital angular momentum matrix:

$$L=\begin{bmatrix} L_c & 0 \\ 0 & L_f \end{bmatrix} \quad (3.15)$$

with L_c and L_f diagonal $n\times n$ and $m\times m$ matrices, respectively, which contain the orbital angular momenta of the $n+m$ channels.

There are for (3.14) $2(n+m)$ independent solutions. The physical solutions must satisfy $n+m$ boundary conditions in the origin and an additional n boundary conditions at infinity for those components, which belong to the permanently confined channels. No other boundary conditions are to be imposed as long as the energy is above all thresholds. In that case there are m-independent physical solutions, which can be found in a straightforward way and lead to an $m\times m$ unitary and symmetric S matrix. Note that in this context by S matrix is understood the scattering matrix for the open two-meson channels.

An explicit expression for the S matrix is derived in Appendix A.

When E is smaller than some of the D_j then the corresponding momenta as defined in (3.4) become purely imaginary. In order to satisfy additional boundary conditions at infinity for those components of the wave function, which belong to the closed meson-meson channels, the imaginary parts of these momenta should be chosen positive. If these values are substituted in (A15), then the submatrix of S corresponding to the remaining open channels is again unitary and takes over the function of the S matrix.

Once $V_{\rm int}$ (3.12) is given, we can calculate the S matrix (A15) and its pole positions in the complex energy plane. Each pole is either identified with a resonance (provided it is close to the real axis) or with a bound state. In this paper we make the approximation that the real part equals its mass and the imaginary part equals half its hadronic width. For bound states with respect to strong decay the poles are on the real axis. The M_1M_2 channels in these cases are closed, but not empty. For instance in our picture a J/ψ meson is represented by a nine-component wave function, which contains besides the confined $c\bar{c}$ channel also closed channels containing pairs of D and D^* mesons or F and F^* mesons.

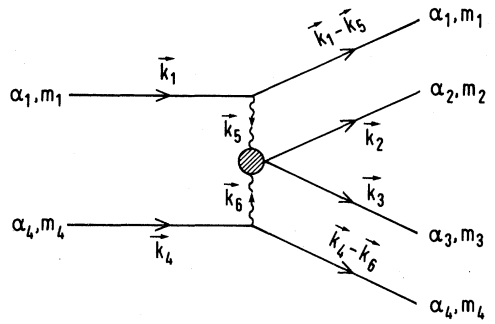

FIG. 3. Diagram of momentum flow for the process described in formula (4.1).

In the present article we will study the vector-meson resonances ($J^{PC}=1^{--}$) and the pseudoscalar mesons ($J^{PC}=0^{-+}$).

IV. THE TRANSITION POTENTIAL

We describe the transitions between the quark-antiquark and the two-meson channels through the creation or annihilation of a quark-antiquark pair in the $^3P_0$ state.[15,16] In the following we treat the quarks nonrelativistically.

Since we deal in this investigation with a wide range of flavor masses, it appears that for phenomenological reasons we have to extend the $^3P_0$ model of Ref. 15. We do this by assuming more structure in the string breaking mechanism. The interaction Hamiltonian which can accommodate our phenomenological needs reads (see also Fig. 3)

$$H_I=\gamma_0\int d^3k_1\cdots d^3k_6\,\delta^3(\vec{k}_2+\vec{k}_3-\vec{k}_5-\vec{k}_6)$$

$$\times\{\tilde{\phi}(\vec{k}_2,\vec{k}_3;\vec{k}_5,\vec{k}_6)[C^{1\ 1\ 0}_{m_{23}\,\mu_{23}\,0}C^{1/2\ 1/2\ 1}_{m_2\ m_3\ \mu_{23}}\mathscr{Y}^{(1)}_{m_{23}}(\vec{k}_2-\vec{k}_3)b^{\dagger}_{\alpha_2,m_2}(\vec{k}_2)d^{\dagger}_{\alpha_3,m_3}(\vec{k}_3)M^{(0)}_{\alpha_2\alpha_3}]$$

$$\times[b^{\dagger}_{\alpha_1,m_1}(\vec{k}_1-\vec{k}_5)b_{\alpha_1,m_1}(\vec{k}_1)d^{\dagger}_{\alpha_4,m_4}(\vec{k}_4-\vec{k}_6)d_{\alpha_4,m_4}(\vec{k}_4)]+\text{H.c.}\}\,. \quad (4.1)$$

Here k_i, m_i, and α_i $(i=1,\ldots,4)$ are the momentum, SU(2)-spin and SU(N)-flavor indices, respectively, of the quarks and antiquarks. Furthermore,

$$\mathscr{Y}^{(1)}_{m_{23}}(\vec{k}_2-\vec{k}_3)=i\,|\,\vec{k}_2-\vec{k}_3\,|\,Y^{(1)}_{m_{23}}\left(\frac{\vec{k}_2-\vec{k}_3}{|\,\vec{k}_2-\vec{k}_3\,|}\right) \tag{4.2a}$$

and $M^{(0)}_{\alpha_2,\alpha_3}$ describes a flavor-singlet quark-antiquark pair. (For typographical reasons we have not distinguished between upper and lower SU(N) indices [see also (5.3)].) Color SU(3) is added in Sec. VI, but omitted here. The dimensionless constant γ_0 describes the strength of the creation and annihilation process. In (4.1) the function $\tilde{\phi}(\vec{k}_2,\vec{k}_3;\vec{k}_5,\vec{k}_6)$ describes the momentum distribution of the created or annihilated $q\bar{q}$ pair (variables $\vec{k}_2$ and $\vec{k}_3$), the momentum transfer between the "spectator" quarks (variables $\vec{k}_5$ and $\vec{k}_6$), and a possible relation between these variables. Note that the special choice

$$\tilde{\phi}(\vec{k}_2,\vec{k}_3;\vec{k}_5,\vec{k}_6)=\delta^{(3)}(\vec{k}_5+\vec{k}_6) \tag{4.2b}$$

leads to the $^3P_0$ model of Ref. 15.

In this paper we use the ansatz

$$\tilde{\phi}(\vec{k}_2,\vec{k}_3;\vec{k}_5,\vec{k}_6)=\tilde{\phi}_{23}(\vec{k}_2,\vec{k}_3)\tilde{\phi}_{56}(\vec{k}_5,\vec{k}_6)\,. \tag{4.3}$$

The incoming quark-antiquark state in the c.m. system is given by

$$|\,\vec{k};s,\mu;\nu\rangle=C^{1/2\ 1/2\ s}_{m_1\ m_4\ \mu}M^{(\nu)}_{\alpha_1,\alpha_4}b^{\dagger}_{\alpha_1,m_1}(\vec{k})d^{\dagger}_{\alpha_4,m_4}(-\vec{k})\,|\,0\rangle\,, \tag{4.4}$$

where $\vec{k}$ is the c.m. momentum, s is the total spin, and ν denotes the SU(N)-flavor state. The latter is described by the flavor matrix M [see (5.3) for a definition].

Similarly for the two-meson state one has

$$|\,\vec{p};s',\mu';\nu_1,\nu_2\rangle=C^{s_1\,s_2\,s'}_{\mu_1\mu_2\mu'}C^{\dagger}_1(\vec{p};s_1,\mu_1;\nu_1)C^{\dagger}_2(-\vec{p};s_2,\mu_2;\nu_2)\,|\,0\rangle\,. \tag{4.5}$$

Here the meson creation operators $C^{\dagger}_i$ are given by

$$C^{\dagger}_1(\vec{p}_1;s_1,\mu_1;\nu_1)=\int d^3q_1d^3q_2\tilde{\psi}^*_1(E(\vec{p}_1),\vec{q}_1,\vec{q}_2)\delta^{(3)}(\vec{q}_1+\vec{q}_2-\vec{p}_1)\ C^{1/2\ 1/2\ s_1}_{m_1\ m_2\ \mu_1}M^{(\nu_1)}_{\beta_1\beta_2}b^{\dagger}_{\beta_1,m_1}(\vec{q}_1)d^{\dagger}_{\beta_2,m_2}(\vec{q}_2)\,, \tag{4.6}$$

$$C^{\dagger}_2(\vec{p}_2;s_2,\mu_2;\nu_2)=\int d^3q_3d^3q_4\tilde{\psi}^*_2(E(\vec{p}_2),\vec{q}_3,\vec{q}_4)\delta^{(3)}(\vec{q}_3+\vec{q}_4-\vec{p}_2)\ C^{1/2\ 1/2\ s_2}_{m_3\ m_4\ \mu_2}M^{(\nu_2)}_{\beta_3\beta_4}b^{\dagger}_{\beta_3,m_3}(\vec{q}_3)d^{\dagger}_{\beta_4,m_4}(\vec{q}_4)\,. \tag{4.7}$$

Here ψ_i $(i=1,2)$ are the internal wave functions of the mesons. Their energy dependence is due to a Lorentz transformation from the meson rest frame to the two-meson center-of-mass frame.

In the following we call the process in Fig. 3 the direct (exchange) process when the mesons with quantum numbers ν_1 (ν_2) and ν_2 (ν_1) are composed by the quarks 1 and 2, respectively, 3 and 4. The direct (exchange) potential V_D (V_E) corresponds to the matrix element of H_I for the direct (exchange) process.

Working out (4.1), using (4.3)–(4.7) we get

$$\langle p';s',\mu';s_1\nu_1,s_2\nu_2\,|\,V_D\,|\,\vec{k};s,\mu;\nu\rangle=-\gamma_0C^{s\ 1\ s'}_{\mu\ \mu_{23}\mu'}C^{1\ 1\ 0}_{m_{23}\ \mu_{23}\ 0}\begin{bmatrix}\frac{1}{2}&\frac{1}{2}&s_1\\ \frac{1}{2}&\frac{1}{2}&s_2\\ s&1&s'\end{bmatrix}\mathrm{Tr}(M^{(\nu_2)^{\dagger}}M^{(\nu_1)^{\dagger}}M^{(\nu)})\tilde{F}_{12,m_{23}}(\vec{p},\vec{k})\,. \tag{4.8}$$

In the derivation of (4.8) we used

$$\sum C^{1/2\ 1/2\ s_1}_{m_1\ m_2\ \mu_1}C^{1/2\ 1/2\ s_2}_{m_4\ m_3\ \mu_2}C^{s_1\ s_2\ s'}_{\mu_1\mu_2\mu'}C^{1/2\ 1/2\ s}_{m_1\ m_4\ \mu}C^{1/2\ 1/2\ 1}_{m_2\ m_3\ \mu_{23}}=C^{s\ 1\ s'}_{\mu\ \mu_{23}\mu'}\begin{bmatrix}\frac{1}{2}&\frac{1}{2}&s_1\\ \frac{1}{2}&\frac{1}{2}&s_2\\ s&1&s'\end{bmatrix}\,. \tag{4.9}$$

Furthermore, we have introduced

$$\tilde{F}_{12,m_{23}}(\vec{p},\vec{k})=2\int d^3q\,\mathscr{Y}^{(1)}_{m_{23}}(\vec{k}-\vec{p}-\vec{q})\tilde{\phi}_{56}(\vec{q}_1-\vec{q})\tilde{\phi}_{23}(\vec{p}-\vec{k}+\vec{q},-\vec{p}+\vec{k}-\vec{q})$$
$$\times\tilde{\psi}^*_1(E_{\vec{p}};\vec{k}-\vec{q},-\vec{k}+\vec{p}+\vec{q})\tilde{\psi}^*_2(E_{\vec{p}};\vec{k}-\vec{p}-\vec{q},-\vec{k}+\vec{q})\,. \tag{4.10}$$

Introducing

$$\vec{\Delta}=\vec{k}-\vec{p},\quad \vec{Q}=\vec{k}+\vec{p}\ , \tag{4.11}$$

we rewrite (4.9) for later use in the form

$$\tilde{F}_{12,m_{23}}(\vec{p},\vec{k})=2\int d^3q\,\mathscr{Y}^{(1)}_{m_{23}}(\vec{\Delta}-\vec{q})\tilde{\phi}_{56}(\vec{q},-\vec{q})\tilde{\phi}_{23}(-\vec{\Delta}+\vec{q},\vec{\Delta}-\vec{q})$$
$$\times\tilde{\psi}^*_1(E_{\vec{p}};-\tfrac{3}{2}\vec{\Delta}+\tfrac{1}{2}\vec{Q}-2\vec{q})\tilde{\psi}^*_2(E_{\vec{p}};\tfrac{3}{2}\vec{\Delta}+\tfrac{1}{2}\vec{Q}-2\vec{q})\ , \tag{4.12}$$

where we have used that in the applications further on we will always assume that the internal wave functions depend on the difference of the momenta only. The transition matrix elements in configuration space are obtained by the Fourier transformation

$$F_{12,m_{23}}(\vec{r}',\vec{r})=\frac{1}{(2\pi)^3}\int\int d^3p\,d^3k\,e^{-i\vec{p}\cdot\vec{r}'}\tilde{F}_{12,m_{23}}(\vec{p},\vec{k})e^{i\vec{k}\cdot\vec{r}}\ . \tag{4.13}$$

In the nonrelativistic limit, using the Gaussian wave function, i.e., ground-state wave functions,

$$\tilde{\psi}_i(\vec{q}_1,\vec{q}_2)=\left[\frac{R_i^2}{\pi}\right]^{3/4}\exp[-\tfrac{1}{8}(\vec{q}_1-\vec{q}_2)^2R_i^2]\ , \tag{4.14}$$

$$\tilde{\phi}_{56}(\vec{k}_5,\vec{k}_6)\sim\exp[-\tfrac{1}{8}(\vec{k}_5-\vec{k}_6)^2r_0^2]\ , \tag{4.15}$$

$$\tilde{\phi}_{23}(\vec{k}_2,\vec{k}_3)\sim 1\ , \tag{4.16}$$

we find in local approximation (i.e., $\vec{Q}=0$) for $r_0\ll R_i$

$$F_{12,m_{23}}(\vec{r}',\vec{r})=\gamma\delta^3(\vec{r}'-\vec{r})\frac{r}{r_0}\exp\left[-\frac{1}{2}\frac{r^2}{r_0^2}\right]Y^{(1)}_{m_{23}}(\hat{r})\ . \tag{4.17}$$

In (4.17) we have accounted for all constants in the transition from γ_0 to γ. Because the expression for $\tilde{F}_{12,m_{23}}(\vec{p},t)$ in (4.12) has a convolutive form we get that in general $F_{12,m_{23}}(\vec{r}',\vec{r})$ is a function of $(1/r_0+1/R_i)$ and so the r_0 parameter in (4.17) is different from that in (4.15). For charmonium and upsilon they will be the same in this paper because then we have $r_0\ll R_i$ (see Sec. VI).

In this paper we will use the form given in (4.17) and generalize it to the relativistic case by making γ apart from flavor also energy dependent.

So, finally we arrive at the configuration-space transition potential

$$\langle\vec{r}';s',\mu';s_1\nu_1,s_2\nu_2\,|\,V_D\,|\,\vec{r};s,\mu;\nu\rangle$$
$$=\gamma\delta^3(\vec{r}'-\vec{r})C^{s\ 1\ s'}_{\mu\ \mu_{23}\ \mu'}C^{1\ 1\ 0}_{m_{23}\ \mu_{23}\ 0}\begin{bmatrix}\frac{1}{2}&\frac{1}{2}&s_1\\ \frac{1}{2}&\frac{1}{2}&s_2\\ s&1&s'\end{bmatrix}\mathrm{Tr}(M^{(\nu_2)^\dagger}M^{(\nu_1)^\dagger}M^{(\nu)})Y^{(1)}_{m_{23}}(\hat{r})\frac{r}{r_0}\exp\left[-\frac{1}{2}\frac{r^2}{r_0^2}\right]\ . \tag{4.18}$$

The potential for states with total angular momenta J,J' and total orbital angular momenta L, L' is for the potential (4.18) given by

$$\langle J',M';L',s';s_1\nu_1,s_2\nu_2\,|\,V_D(r)\,|\,J,M;L,s\,\rangle$$
$$=C^{L'\ s'\ J'}_{m'\ \mu'\ M'}C^{L\ s\ J}_{m\ \mu\ M}\int d\Omega_{r'}Y^{(L')^*}_{m'}(\hat{r}')\int d\Omega_r Y^{(L)}_m(\hat{r})\langle\vec{r}';s'\mu',s_1\nu_1,s_2\nu_2\,|\,V\,|\,\vec{r};s,\mu;\nu\rangle$$
$$=\gamma\left[\frac{3(L+L'+1)}{8\pi(2L'+1)}\right]^{1/2}\begin{bmatrix}\frac{1}{2}&\frac{1}{2}&s_1\\ \frac{1}{2}&\frac{1}{2}&s_2\\ s&1&s'\end{bmatrix}\begin{bmatrix}L&1&L'\\ s&1&s'\\ J&0&J\end{bmatrix}\delta_{J'J}\delta_{M'M}\mathrm{Tr}(M^{(\nu_2)^\dagger}M^{(\nu_1)^\dagger}M^{(\nu)})\frac{r}{r_0}\exp\left[-\frac{1}{2}\frac{r^2}{r_0^2}\right]\ . \tag{4.19}$$

In the derivation of (4.19) we used

$$\int d\Omega\,Y^{(L')^*}_{m'}(\hat{r})Y^{(1)}_{m_{23}}(\hat{r})Y^{(L)}_m(\hat{r})=\left[\frac{3(2L+1)}{4\pi(2L'+1)}\right]^{1/2}C^{L\ 1\ L'}_{0\ 0\ 0}C^{L\ 1\ L'}_{m\ m_{23}\ m'} \tag{4.20}$$

and the identity

$$\sum C^{L's'J'}_{m'\mu'M'} C^{Lsj}_{m\mu M} C^{s\,1\,s'}_{\mu\mu_{23}\mu'} C^{1\,1\,0}_{m_{23}\mu_{23}0} C^{L\,1\,L'}_{m\,m_{23}\,m'} = \begin{bmatrix} L & 1 & L' \\ s & 1 & s' \\ J & 0 & J \end{bmatrix} \delta_{J'J}\delta_{M'M} \,. \tag{4.21}$$

Because (4.1) is the nonrelativistic interaction Hamiltonian, the potential (4.19) can be used directly in the partial-wave Schrödinger equation (3.14).

The contribution of the exchange process to the transitions is included implicitly in the next section [see Eq. (5.4)].

V. TRANSITION MATRIX ELEMENTS

In this section we present tables for the $O(3)\times SU(2)_{spin}\times SU(N)_{flavor}$ part of the potential (4.18). We consider processes of the form [(3.1) and Fig. 3]

$$V_{int}:\ q_1+\bar{q}_2 \rightleftarrows (q_1\bar{q})_{M_1}+(q\bar{q}_2)_{M_2} \,. \tag{5.1}$$

The orbital angular momenta and spins of the confined channels $q_1+\bar{q}_2$ and of the meson channels M_1+M_2 are denoted by l, L, s, and S, respectively, and the spins of the mesons M_1 and M_2 by s_1 and s_2, respectively. The total angular momentum of the system is denoted by J. With these definitions the $O(3)\times SU(2)_{spin}$ part of (4.18) for the transitions (5.1) is given by

$$\langle q_1+\bar{q}_2 \,|\, V_{int} \,|\, M_1+M_2 \rangle \sim \left[\frac{3(l+L+1)}{2(2L+1)}\right]^{1/2} \begin{bmatrix} l & 1 & L \\ s & 1 & S \\ J & 0 & J \end{bmatrix} \begin{bmatrix} \frac{1}{2} & \frac{1}{2} & s_1 \\ \frac{1}{2} & \frac{1}{2} & s_2 \\ s & 1 & S \end{bmatrix} . \tag{5.2}$$

The normalization of the matrix elements in (5.2) is such that the sum of the squares of the couplings of one $q\bar{q}$ channel to all scattering channels equals one.

In Ref. 2 we observed that in our model for the $J^{PC}=1^{--}$ mesons the mixing between S states and D states is small. For simplicity we shall drop the $l=2$ permanently closed $q_1+\bar{q}_2$ channel in the present investigation for all mesons. The matrix elements (5.2) which are relevant in this paper ($l=0$ and thus $J=s$ and $L=1$) are summarized in Table II.

TABLE II. $O(3)\times SU(2)_{spin}$ part of the coupling strengths $|\langle \text{meson}+\text{meson} \,|\, V_{int} \,|\, \text{meson}\rangle|^2$.

s \ S_1, S_2, S	0, 0, 0	0, 1, 1	1, 0, 1	1, 1, 0	1, 1, 1	1, 1, 2
0		$\frac{1}{4}$	$\frac{1}{4}$		$\frac{1}{2}$	
1	$\frac{1}{12}$	$\frac{1}{6}$	$\frac{1}{6}$	$\frac{1}{36}$		$\frac{5}{9}$

A further restriction is the assumption that only $u\bar{u}$, $d\bar{d}$, and $s\bar{s}$ pairs are created or annihilated in the process (5.1). This is not unreasonable since the coupling of meson channels and confined channels, which communicate via the creation or annihilation of $c\bar{c}$ and $b\bar{b}$ pairs, is highly suppressed, because the thresholds in the scattering channels are at much higher energies. For the $q\bar{q}$ pair in (5.1) we have chosen exact $SU(3)_{flavor}$ symmetry, which implies that the matrix elements $\langle q\bar{q} \,|\, 0\rangle$ and $\langle 0 \,|\, q\bar{q}\rangle$ as well as the transition radius r_0 in (4.16) are the same for nonstrange and strange quarks.

As mentioned before we consider only those two-particle-scattering channels, which contain the pseudoscalar mesons π, η, η', K, D, F, B, and G and the vector mesons ρ, ω, ϕ, K^*, D^*, F^*, B^*, and G^*. Here we have denoted the open-b-flavor analogs of the well-known open-charm mesons D, D^*, F, and F^*, by B, B^*, and G, and G^*. Of these mesons only the B meson has been found[23] in the energy region around 5.2 GeV. For the masses of the B^*, G, and G^* mesons we have to make some estimates inspired by the splittings between the open-charm mesons. Moreover, we take ideal mixing for the η, η', ω, and ϕ mesons.

It is convenient to define the conventional 5×5 matrices $P_{\alpha\beta}$ and $V_{\alpha\beta}$ for the $24+1$ pseudoscalar and vector multiplets of $SU(5)_{flavor}$ (see also Ref. 16):

$$P = \begin{bmatrix} \frac{1}{\sqrt{2}}(\eta+\pi^0) & \pi^+ & K^+ & \bar{D}^0 & B^+ \\ \pi^- & \frac{1}{\sqrt{2}}(\eta-\pi^0) & K^0 & D^- & B^0 \\ K^- & \bar{K}^0 & \eta' & F^- & G^0 \\ D^0 & D^+ & F^+ & \eta_c & - \\ B^- & \bar{B}^0 & \bar{G}^0 & - & \eta_b \end{bmatrix} , \tag{5.3}$$

$$V = \begin{bmatrix} \frac{1}{\sqrt{2}}(\omega+\rho^0) & \rho^+ & K^{*+} & \bar{D}^{*0} & B^{*+} \\ \rho^- & \frac{1}{\sqrt{2}}(\omega-\rho^0) & K^{*0} & D^{*-} & B^{*0} \\ K^{*-} & \bar{K}^{*0} & \phi & F^{*-} & G^{*0} \\ D^{*0} & D^{*+} & F^{*+} & \psi & - \\ B^{*-} & \bar{B}^{*0} & \bar{G}^{*0} & - & \Upsilon \end{bmatrix} .$$

TABLE III. Couplings of confined and free channels for η_c and ψ.

$\eta_c(c\bar{c})$	$\psi(c\bar{c})$		Spin
	$\frac{1}{18}$	DD	0
$\frac{1}{3}$	$\frac{2}{9}$	DD^*	1
	$\frac{1}{54}$	D^*D^*	0
$\frac{1}{3}$		D^*D^*	1
	$\frac{10}{27}$	D^*D^*	2
	$\frac{1}{36}$	FF	0
$\frac{1}{6}$	$\frac{1}{9}$	FF^*	1
	$\frac{1}{108}$	F^*F^*	0
$\frac{1}{6}$		F^*F^*	1
	$\frac{5}{27}$	F^*F^*	2

If in (5.1) $q_1+\bar{q}_2$ is the member A_{ij} of one of these multiplets and M_1 and M_2 are the members B_{kl} and C_{mn} of the multiplets P or V, then the relative coupling strengths can be found from

$$\frac{1}{\sqrt{2}\,\mathrm{Tr}P}\langle B_l^k C_n^m \,|\, \mathrm{Tr}A^+[BPC+\sigma(A,B,C)CPB]\,|\,A_j^i\rangle\ , \tag{5.4}$$

where P is a projection operator and where $\sigma(A,B,C)$ is given by the product of the charge-conjugation parities of the three mesons A, B, and C. By taking $P=\mathrm{diag}(1,1,1,0,0)$ in (5.4) we select those couplings, which are connected with the creation or annihilation of light-quark pairs.

The expression (5.4) is appropriate for all charge modes of each meson. For practical reasons we put together all two-meson channels with the same (or nearly the same) thresholds.

In Tables III, IV, and V the total $\mathrm{O(3)}\times\mathrm{SU(2)_{spin}}\times\mathrm{SU(5)_{flavor}}$ relative coupling strengths are shown for the ψ and η_c, for the D, D^*, F, and F^* mesons and for the light mesons, respectively. The results for the Υ and η_b are identical to the results for the ψ and η_c.

Notice that the couplings of a particle to all its decay channels add up to one, except for the ω and ϕ mesons. This deviation originates from the fact that we have selected only a special class of decay products. In this paper we have renormalized the couplings of the ω and the ϕ.

VI. COLOR SPLITTING AND PHENOMENOLOGICAL REFINEMENTS

In this section we present the precise form of the transition potential which we have used in our calculations. The main ingredients are simplicity and phenomenology.

The radial dependence $g(r)$ of the potential given in (A6) can be read off from the expression (4.18) to be

$$g(r)=\tilde{g}\frac{r}{r_0}\exp\left[-\frac{1}{2}\frac{r^2}{r_0^2}\right]\ , \tag{6.1}$$

where $\tilde{g}$ is a fit parameter.

In order to fit simultaneously the light and heavy mesons, the transition radius r_0 in (6.1) must be dependent on the flavor masses of the quarks of these states. This might be interpreted as a consequence of the dependence of the momentum-transfer distribution (4.14) on the quark masses m_{q_1} and m_{q_4} (see Fig. 3). For simplicity we have chosen

$$r_0=\left[\frac{m_{q_1}m_{q_4}}{m_{q_1}+m_{q_4}}\right]^{-1/2}\omega^{-1/2}\rho_0\ , \tag{6.2}$$

where the dimensionless constant ρ_0 is the same for all mesons.

For phenomenological reasons we also need a suppression of the coupling to scattering channels with a high threshold, because the kinematical suppression is not sufficient to reduce their influence. The effect is mainly seen in the resulting hadronic widths, which otherwise are too small compared with experiment.

As we have approximated the nonlocal transition potential by an effective local one, this can be done by taking the elements of the matrix $\bar{V}_{\mathrm{int}}$ in (A6) to be dependent on the threshold value of the corresponding scattering channel:

$$(\bar{V}_{\mathrm{int}})_{ij}\sim D_j^{-1/2}=(m_{M_{1,j}}+m_{M_{2,j}})^{-1/2}\ , \tag{6.3a}$$

where $(\bar{V}_{\mathrm{int}})_{ij}$ describes the transition from the ith permanent closed channel ($i=1$ in this paper, because we take only the $l=0$ $q\bar{q}$ channel into account) to the jth two-meson channel and where $m_{M_{kj}}$ ($k=1,2$) are the masses of the two mesons. However, the choice (6.3a) would mutilate the effective coupling constant, since thresholds for light mesons differ drastically from thresholds for heavy mesons. For this reason we alter (6.3a) such that for thresholds at the resonance position, the effective coupling is the same for all mesons:

$$(\bar{V}_{\mathrm{int}})_{ij}\sim\left[\frac{E}{D_j}\right]^{1/2}\ . \tag{6.3b}$$

This introduces an energy dependence in the potential, because E is the energy in the Schrödinger

TABLE IV. Couplings of confined and free channels for D, D^*, F, and F^* mesons.

$D(c\bar{n})$	$D^*(c\bar{n})$	$F(c\bar{s})$	$F^*(c\bar{s})$		Spin
	$\frac{1}{72}$			$D\eta$	0
	$\frac{1}{24}$			$D\pi$	0
			$\frac{1}{18}$	DK	0
	$\frac{1}{36}$			FK	0
			$\frac{1}{36}$	$F\eta'$	0
$\frac{1}{24}$	$\frac{1}{36}$			$D\omega$	1
$\frac{1}{8}$	$\frac{1}{12}$			$D\rho$	1
		$\frac{1}{6}$	$\frac{1}{9}$	DK^*	1
$\frac{1}{12}$	$\frac{1}{18}$			FK^*	1
		$\frac{1}{12}$	$\frac{1}{18}$	$F\phi$	1
$\frac{1}{24}$	$\frac{1}{36}$			$D^*\eta$	1
$\frac{1}{8}$	$\frac{1}{12}$			$D^*\pi$	1
		$\frac{1}{6}$	$\frac{1}{9}$	D^*K	1
$\frac{1}{12}$	$\frac{1}{18}$			F^*K	1
		$\frac{1}{12}$	$\frac{1}{18}$	$F^*\eta'$	1
	$\frac{1}{216}$			$D^*\omega$	0
$\frac{1}{12}$				$D^*\omega$	1
	$\frac{5}{54}$			$D^*\omega$	2
	$\frac{1}{72}$			$D^*\rho$	0
$\frac{1}{4}$				$D^*\rho$	1
	$\frac{5}{18}$			$D^*\rho$	2
			$\frac{1}{54}$	D^*K^*	0
		$\frac{1}{3}$		D^*K^*	1
			$\frac{10}{27}$	D^*K^*	2
	$\frac{1}{108}$			F^*K^*	0
$\frac{1}{6}$				F^*K^*	1
	$\frac{5}{27}$			F^*K^*	2
			$\frac{1}{108}$	$F^*\phi$	0
		$\frac{1}{6}$		$F^*\phi$	1
			$\frac{5}{27}$	$F^*\phi$	2

equation (3.14). However, the resulting S matrix is still analytic.

A possible contribution to this suppression may come from a boost of the internal wave functions of the final-state mesons from the rest frame of one meson to the c.m. frame. However, such effects are model dependent and depend on how one takes into account a wave function for the $^3P_0$ pair. Besides, a complete account of this boost introduces extra non-local effects in the transition potential.

Since also the pseudoscalar mesons are treated in this article, it is necessary to describe the mechanism which gives the mass splittings between the pseudoscalar and the vector mesons. In commonly accepted models this is accomplished by means of a correction term which stems from a one-gluon-exchange potential. For the mesons under consideration the splitting has the form[24,8]

TABLE V. Couplings of confined and free channels for the light mesons.

η	η'	π	K	ω	ϕ	ρ	K^*		Spin
							$\frac{1}{72}$	$\eta\ K$	0
				$\frac{1}{9}$				$\eta\ \omega$	1
						$\frac{1}{9}$		$\eta\ \rho$	1
			$\frac{1}{24}$				$\frac{1}{36}$	$\eta\ K^*$	1
							$\frac{1}{36}$	$\eta'\ K$	0
					$\frac{2}{9}$			$\eta'\ \phi$	1
			$\frac{1}{12}$				$\frac{1}{18}$	$\eta'\ K^*$	1
						$\frac{1}{18}$		$\pi\ \pi$	0
							$\frac{1}{24}$	$\pi\ K$	0
						$\frac{1}{9}$		$\pi\ \omega$	1
		$\frac{1}{3}$		$\frac{1}{3}$				$\pi\ \rho$	1
			$\frac{1}{8}$				$\frac{1}{12}$	$\pi\ K^*$	1
				$\frac{1}{36}$	$\frac{1}{18}$	$\frac{1}{36}$		$K\ K$	0
			$\frac{1}{24}$				$\frac{1}{36}$	$K\ \omega$	1
			$\frac{1}{12}$				$\frac{1}{18}$	$K\ \phi$	1
			$\frac{1}{8}$				$\frac{1}{12}$	$K\ \rho$	1
$\frac{1}{6}$	$\frac{1}{3}$	$\frac{1}{6}$		$\frac{1}{9}$	$\frac{2}{9}$	$\frac{1}{9}$		$K\ K^*$	1
$\frac{1}{6}$								$\omega\ \omega$	1
		$\frac{1}{3}$						$\omega\ \rho$	1
							$\frac{1}{216}$	$\omega\ K^*$	0
			$\frac{1}{12}$					$\omega\ K^*$	1
							$\frac{5}{54}$	$\omega\ K^*$	2
	$\frac{1}{3}$							$\phi\ \phi$	1
							$\frac{1}{108}$	$\phi\ K^*$	0
			$\frac{1}{6}$					$\phi\ K^*$	1
							$\frac{5}{27}$	$\phi\ K^*$	2
						$\frac{1}{54}$		$\rho\ \rho$	0
$\frac{1}{2}$								$\rho\ \rho$	1
						$\frac{10}{27}$		$\rho\ \rho$	2
							$\frac{1}{72}$	$\rho\ K^*$	0
			$\frac{1}{4}$					$\rho\ K^*$	1
							$\frac{5}{18}$	$\rho\ K^*$	2
				$\frac{1}{108}$	$\frac{1}{54}$	$\frac{1}{108}$		K^*K^*	0
$\frac{1}{6}$	$\frac{1}{3}$	$\frac{1}{6}$						K^*K^*	1
				$\frac{5}{27}$	$\frac{10}{27}$	$\frac{5}{27}$		K^*K^*	2

$$\Delta E_{\text{color}} \sim \frac{\vec{s}_q \cdot \vec{s}_{\bar{q}}}{m_q m_{\bar{q}}} |\psi(0)|^2 , \tag{6.4}$$

where $\psi(0)$ is the $q\bar{q}$ wave function at the origin and where ($m_{\bar{q}}$) m_q and ($s_{\bar{q}}$) s_q are the (anti-) quark mass and the (anti-) quark spin, respectively.

For harmonic-oscillator functions (6.4) would result in a term

$$\Delta E_{\text{color}} \sim \frac{\vec{s}_q \cdot \vec{s}_{\bar{q}}}{m_q m_{\bar{q}}} \left[\frac{m_q m_{\bar{q}}}{m_q + m_{\bar{q}}} \right]^{3/2} \omega^{3/2} . \tag{6.5}$$

This could be taken as a constant correction term in the direct $q\bar{q}$ potential, but this has the unwanted consequence that radial excitations would have about the same mass splittings as the ground states, contrary to experiment and contrary to earlier results,[2] which showed that in this model the wave functions at the origin of the radial excitations are smaller than the wave functions at the origin of the corresponding ground state and therefore should give smaller mass splittings according to (6.4). However, we notice that a similar term, taken as a correction of the transition potential has to second order in perturbation theory an effect comparable to (6.5), but has the advantage that then the proper wave function is taken into account. Therefore, we use a transition potential of the form

$$g(r)[\bar{V}_{\text{int}}]_{ij} = \tilde{g} c_{ij} \left[\frac{E}{D} - g_c \sqrt{\omega} \frac{(m_q m_{\bar{q}})^{1/2}}{(m_q + m_{\bar{q}})^{3/2}} \vec{s}_q \cdot \vec{s}_{\bar{q}} \right]^{1/2} \frac{r}{r_0} \exp\left[-\frac{1}{2} \frac{r^2}{r_0^2} \right] . \tag{6.6}$$

Also a word must be said about the consequences of the nonrelativistic approximation to the relativistic formulation (3.11).

In those scattering channels, for which the thresholds are far below a resonance position, it is clearly wrong to do calculations with nonrelativistic kinematics. In Sec. III it is shown how relativistic kinematics might be accounted for in a Schrödinger equation. Our strategy has been as follows: In open scattering channels relativistic kinematics is used:

$$\begin{aligned} k^2 &= \tfrac{1}{4} E^{-2} [E^2 - (m_{M_1} + m_{M_2})^2] \\ &\quad \times [E^2 - (m_{M_1} - m_{M_2})^2] , \\ \mu(E) &= \tfrac{1}{4} E^{-3} [E^4 - (m_{M_1} + m_{M_2})^2 (m_{M_1} - m_{M_2})^2] . \end{aligned} \tag{6.7}$$

Closed channels are treated nonrelativistically:

$$\begin{aligned} k^2 &= 2\mu(E - m_{M_1} - m_{M_2}) , \\ \mu &= (m_{M_1} + m_{M_2})^{-1} m_{M_1} m_{M_2} . \end{aligned} \tag{6.8}$$

This procedure does certainly not yield an S matrix with the usual analyticity properties. However, for any particular energy region, it is possible to do the choices (6.7) and (6.8) beforehand. This restores piecewise analyticity and one can figure out afterwards whether the different solutions for different energy regions overlap in adjacent domains. This has been checked to be the case.

The choice (6.8) below threshold is necessary because of two annoying features of analytic continuation of the expressions (6.7): (a) For $E^2 < (m_{M_1} + m_{M_2}) | m_{M_1} - m_{M_2} |$ the reduced mass becomes negative. (b) Below the pseudothreshold, i.e., for $E < | m_{M_1} - m_{M_2} |$, the exponential wave

TABLE VI. Masses (in GeV) of the mesons used to fit the parameters, and their widths (in MeV).

Particle	Theoretical mass	Experimental mass	Theoretical width	Experimental width
ρ	0.76	0.770	150	158
ρ'	1.29	1.25	30	~125
ρ''	1.59	1.6	75	~200
K	0.50	0.496		
K^*	0.93	0.895	48	50
ϕ	1.03	1.020	5	4
ϕ'	1.53	1.65	10	~100
ϕ''	1.87	1.9	62	~400
J/ψ	3.10	3.095		
ψ'	3.67	3.684		
ψ''	4.05	4.030	21	52
ψ'''	4.41	4.414	89	43
Υ	9.41	9.433		
Υ'	10.00	9.993		
Υ''	10.40	10.324		
Υ'''	10.77	10.548	37	?

TABLE VII. Masses (in GeV) of the remaining ground-state mesons.

Particle	Theoretical mass	Experimental mass
π	0.40	0.138
η (η_n)	0.39	0.549
η' (η_s)	0.60	0.958
ω	0.84	0.783
D	1.66	1.866
F	1.75	2.030
D^*	1.94	2.007
F^*	2.04	2.140
η_c	2.83	2.981
η_c'	3.61	3.592

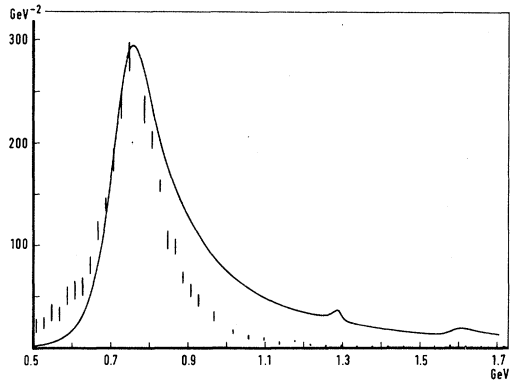

FIG. 4. Elastic p-wave $\pi\pi$ cross section.

functions in terms of k no longer satisfy the proper boundary condition at infinity.

VII. RESULTS, COMPARISON WITH EXPERIMENT, AND DISCUSSION

The parameters of the model are (a) the harmonic-oscillator frequency ω, which approximately can be read off from the experimental radial spectra (see Fig. 1) to be about 180 MeV; (b) the coupling constants $\tilde{g}$ and g_c, which determine, respectively, the overall coupling strength of the $q\bar{q}$ channel to the scattering channels, and the mass splittings between the pseudoscalars and the vectors; (c) the dimensionless transition radius ρ_0, at which position the transition potential has its maximum; and (d) the constituent quark masses $m_n \equiv m_u = m_d$, m_s, m_c, and m_b.

A least-squares fit to the meson masses, which are shown in Table VI, gives for these parameters the results

$$\omega = 190 \text{ MeV}, \rho_0 = 0.56 ,$$

$$\tilde{g}^2/4\pi = 7.59 , \quad g_c = 5.47 ,$$

$$m_n = 406 \text{ MeV}, \quad m_s = 508 \text{ MeV},$$

$$m_c = 1562 \text{ MeV}, m_b = 4724 \text{ MeV} .$$

With this set of parameters we obtain for the other mesons the results as shown in Table VII. At this point we should remark that for the masses of resonances we take the real parts of the poles in the S matrix, except for the $\rho(770)$. The reason to do so is the observation that for nearly all the meson resonances considered the real part of the pole energy roughly coincides with the maximum in the calculated total cross section. However, for the $\rho(770)$, being a very well established resonance, we have taken the more accurate value of the peak in the cross section (depicted in Fig. 4), which is about 25 MeV higher than the pole value, due to the large width and the relatively low mass of the ρ.

The total widths of the meson resonances, for which we take twice the distance of the pole to the real axis, are summarized in Table VI as well. Some of the radial excitations, however, exhibit structures in the theoretical P-wave cross section, which clearly carry a great deal of background coming from the ground-state resonance pole (see Fig. 4). This makes a direct comparison of imaginary parts of pole positions and widths of cross-section peaks very difficult.

Comparing the calculated masses with the more or less established experimental ones we see a good agreement for the radial spectra, except for the Υ''', but a clear discrepancy for the π, the η's, and the open-charm mesons. The relatively low-lying Υ''' state, which does not fit in our equal spacing scheme, is possibly an indication for the presence of a short-range term in the quark-antiquark central potential, becoming important for very heavy and thus small systems. Such an extra term could indeed make the level splittings decrease going to higher radial excitations. As for the η, the η', and the η_c we note that these isosinglet states, having quantum numbers $J^{PC}=0^{-+}$, can annihilate into two gluons, which could give rise to an effective repulsive quark-antiquark potential, thereby lifting the masses of these particles.[24] Moreover, in our model such an effect would be roughly proportional to $m_q^{-1/2}$, where m_q is the quark mass, so the shifts of the η and η' would be some two or three times the shift of the η_c, which is about what is needed. Apart from this, deviations from the assumed ideal mixing could give rise to additional changes of the masses of especially the η and the η'. Investigations on a dynamical incorporation of such mixing effects in the model are being done. The too small results for the masses of the D, D^*, F, and F^* mesons may be due to the nonrelativistic treatment of closed scattering channels, which differs substantially from

the relativistic approach above threshold, because for these particles several pseudothresholds lie close to the physical masses. Then these open-charm states consisting of quarks with highly unequal masses might have a different effective decay coupling constant. An adjustment of this parameter only for the open-charm systems leads to a good agreement with the data. Finally, for the π meson, having a mass much smaller than its binding energy, the approximations which have been made with respect to the coupling mechanism and the color splitting might have led to deviations, moderate compared with this binding energy, but very large compared with the actual rest mass. Moreover, the physical π meson could in principle be a mixture of a $q\bar{q}$ state and a Goldstone boson.

Turning to the hadronic decay widths we see very good results for the ρ, K^*, and ϕ, but too small ones for the ρ and ϕ radial excitations (note at this point the observations above). For the latter states, however, possible decay channels of a type not considered in this investigation, such as decays into internally excited mesons, might add substantially to the hadronic decay widths. The $\rho'(')(1600)$, for example, decays mainly into $A_1\pi$ in a relative s wave, where A_1 denotes an $I^GJ^{PC}=1^-1^{++}$ state with internal $l=1$.[25] Such decay channels can be incorporated in the model though it will lead to a proliferation of components in our multichannel formalism. This will be studied in the future.

In conclusion, we examine the calculated elastic p-wave $\pi\pi$ cross section in the energy region between 0.5 and 1.7 GeV. The very pronounced peak of the ρ resonance at 760 MeV has a height of 295 GeV^{-2} (115 mb), as it should have because of unitarity, and a width of 180 MeV. The rather small bumps at the positions of the assumed ρ' and ρ'' resonances are far below the unitarity limit, showing the occurrence of competing inelastic channels like $\rho\omega$, $K\bar{K}$, and $\rho\rho$ (for the ρ''). The vagueness of these structures in the $\pi\pi$ cross section might explain the experimental difficulties in establishing these states, in particular the $\rho'(1250)$.

VIII. CONCLUSIONS

The model which has been extensively described in this paper involves an efficient and practical scheme to incorporate strong decay in a quark model of mesons. In the first, rather simplistic, version of the model[2] good results for the spectra of charmonium and b-quarkonium could be produced already, but there the calculated hadronic decay widths turned out to be unrealistically small. In this article the model has been refined and extended in order to make it applicable to a wide variety of $q\bar{q}$ systems. The most significant modification is the introduction of a far more realistic transition potential, which in local approximation can be derived from the $^3P_0$ model. A rapidly converging analytic approximation scheme is given which is very convenient for limiting the computer time needed for the tracing of bound-state and resonance poles. Further, in order to be able to do reliable calculations in the light-meson sector, we perform kinematically relativistic adaptions of the equations. Finally, for the simultaneous handling of pseudoscalar and vector mesons, color splitting is introduced.

The results for the masses and widths of the mesons as produced by the model in its present stage are rather promising. The model can be extended as indicated in Sec. VII and work is in progress to implement improvements: (i) inclusion of additional decay channels involving orbitally excited mesons, (ii) inclusion of two-gluon annihilation and mixing effects of the η mesons, (iii) introduction of final-state interactions, and (iv) modification of the inner region of the confining potential.

In conclusion, our work indicates that results from models not dealing with strong decay have to be reconsidered. In particular we have shown that a harmonic-oscillator spectrum with the same level splittings of all quarkonia can be distorted by strong decay such as to give the physical spectra.

Spectroscopy and scattering features are described within the same model.

ACKNOWLEDGMENTS

We wish to thank the members of the Institute for Theoretical High-Energy Physics at Nijmegen for many useful discussions. This work is part of the research program of the Stichting voor Fundamenteel Onderzoek der Materie (F.O.M.), financially supported by the Nederlandse Organizatie voor Zuiver Wetenschappelijk Onderzoek (Z.W.O.).

APPENDIX

The method we have chosen to solve Eq. (3.14) is the following: First we write for (3.14) the integral equation

$$\phi(r)=\phi_0(r)+\int_0^\infty dr' G(r,r')2\mu(E)\begin{bmatrix} 0 & V_{\mathrm{int}}(r') \\ V_{\mathrm{int}}^T(r') & 0 \end{bmatrix}\phi(r') . \tag{A1a}$$

In (A1a) the Green's function $G(r,r')$ is a solution of

$$\left[-\frac{d^2}{dr^2}+\frac{L(L+1)}{r^2}+2\mu(E)\begin{bmatrix}V_c(r) & 0\\ 0 & V_f(r)\end{bmatrix}-\vec{k}^{\,2}(E)\right]G(r,r')=-\delta(r-r') \tag{A1b}$$

and ϕ_0 a solution of

$$\left[-\frac{d^2}{dr^2}+\frac{L(L+1)}{r^2}+2\mu(E)\begin{bmatrix}V_c(r) & 0\\ 0 & V_f(r)\end{bmatrix}-\vec{k}^{\,2}(E)\right]\phi_0(r)=0\ . \tag{A1c}$$

The integrand in (A1) is sufficiently well behaved in order to allow us to approximate the integral in (A1) by a sum ($r_0=0<r_1<r_2<\cdots$)

$$\phi(r)=\phi_0(r)+\sum_{i=1}^{\infty}\Delta(r_i)G(r,r_i)2\mu(E)\begin{bmatrix}0 & V_{\rm int}(r_i)\\ V_{\rm int}^T(r_i) & 0\end{bmatrix}\phi(r_i)\ , \tag{A2}$$

where $\Delta(r_i)=r_i-r_{i-1}$.

The sum in (A2) can be terminated after N terms for practical purposes and can be written as an integral:

$$\phi(r)=\phi_0(r)+\int_0^{\infty}dr'\Delta(r')G(r,r')2\mu(E)\begin{bmatrix}0 & V_{\rm int}(r')\\ V_{\rm int}^T(r') & 0\end{bmatrix}\phi(r')\sum_{i=1}^{N}\delta(r'-r_i)\ . \tag{A3}$$

Finally the integral equation (A3) can again be written as a differential equation:

$$\left[-\frac{d^2}{dr^2}+\frac{L(L+1)}{r^2}+2\mu(E)\tilde{V}(r)-\vec{k}^{\,2}(E)\right]\phi(r)=0\ , \tag{A4}$$

where the potential $\tilde{V}(r)$ is defined by

$$\tilde{V}(r)=\sum_{i=1}^{N}\Delta(r_i)\begin{bmatrix}0 & V_{\rm int}(r_i)\\ V_{\rm int}^T(r_i) & 0\end{bmatrix}\delta(r-r_i)\ . \tag{A5}$$

For simplicity we absorb the $\Delta(r_i)$ in the off-diagonal term by the definition [using (3.9)]

$$\Delta(r_i)V_{\rm int}(r_i)\equiv\frac{1}{N-1}g(r_i)\frac{M_c^{-1}}{r_0}\bar{V}_{\rm int}\ . \tag{A6}$$

In (A6) we assumed that the radial dependence of the transition potential is the same for all matrix elements, $\bar{V}_{\rm int}$ being an $n\times m$ matrix without r dependence and $g(r)$ a simple function of r. Equation (A4) can be solved analytically.

Let us define the following diagonal matrices: an $n\times n$ radial quantum number matrix u, which through (3.13), (3.14), and (3.15) is given by

$$E=\omega(2u+L_c+\tfrac{3}{2})+C\ ; \tag{A7}$$

the $n\times n$ confluent hypergeometric function matrices

$$\phi(-u,L_c+\tfrac{3}{2};M_c\omega r^2)\ \text{ and }\ \psi(-u,L_c+\tfrac{3}{2};M_c\omega r^2) \tag{A8}$$

which are self-evident generalizations of the ϕ and ψ functions defined in Bateman, Chap. VI;[26] the corresponding regular and irregular solutions of the uncoupled wave equation:

$$F(u,L_c;x)=x^{L_c+1}e^{-x^2/2}\frac{\phi(-u,L_c+\frac{3}{2};x^2)}{\Gamma(L_c+\frac{3}{2})} \tag{A9}$$

and

$$G(u,L_c;x)=x^{L_c+1}e^{-x^2/2}\psi(-u,L_c+\tfrac{3}{2};x^2);$$

the $m\times m$ velocity matrix

$$v=M_f^{-1}k\ ; \tag{A10}$$

and $m\times m$ matrices, which are generalizations of the spherical Bessel, Neuman, and Hankel functions

$$J(L_f,kr)=krj_{L_f}(kr)\ ,$$

$$N(L_f,kr)=krn_{L_f}(kr)\ , \tag{A11}$$

and

$$H^{(1,2)}(L_f,kr)=J(L_f,kr)\pm iN(L_f,kr)\ .$$

Furthermore, it is necessary to introduce the $(2n+2m)\times(2n+2m)$ matrices

$$X(r_i)=\begin{bmatrix} I_{2n\times 2n} & \dfrac{1}{N-1}g(r_i)[M_c\omega]^{1/2}\dfrac{\Gamma(-u)}{r_0}O_1(u,L,k,r_i) \\ \dfrac{-2}{N-1}g(r_i)M_c^{-1}M_f\dfrac{k^{-1}}{r_0}O_2(u,L,k,r_i) & I_{2m\times 2m} \end{bmatrix},$$

where the $2n\times 2m$ matrix O_1 and the $2m\times 2n$ matrix O_2 are defined by

$$O_1(u,L,k,r_i)=\begin{bmatrix} G(u,L_c;[M_c\omega]^{1/2}r_i) \\ -F(u,L_c;[M_c\omega]^{1/2}r_i) \end{bmatrix}\bar{V}_{\rm int}(J(L_f,kr_i),N(L_f,kr_i))$$

and

$$O_2(u,L,k,r_i)=\begin{bmatrix} N(L_f,kr_i) \\ -J(L_f,kr_i) \end{bmatrix}\bar{V}^T_{\rm int}(F(u,L_c;[M_c\omega]^{1/2}r_i),G(u,L_c;[M_c\omega]^{1/2}r_i))\ .$$

We also define four $n\times n$ matrices $X^{(N)}_{ij}$ $(i,j=1,2)$, four $n\times m$ matrices $X^{(N)}_{ij}$ $(i=1,2,;\ j=3,4)$, four $m\times n$ matrices $X^{(N)}_{ij}$ $(i=3,4,;\ j=1,2)$, and four $m\times m$ matrices $X^{(N)}_{ij}$ $(i,j=3,4)$ by

$$X^{(N)}_{ij}=[X(r_N)\cdots X(r_1)]_{ij}\quad (i,j=1.,\ldots,4)\ . \tag{A13}$$

Finally we define

$$Z_{L_f}(E)=[-X^{(N)}_{41}X^{(N)-1}_{11}X^{(N)}_{13}+X^{(N)}_{43}][-X^{(N)}_{31}X^{(N)-1}_{11}X^{(N)}_{13}+X^{(N)}_{33}]^{-1}\ . \tag{A14}$$

With (A10) and (A14) the S matrix reads

$$S_{L_f}(E)=v^{1/2}[1-iZ_{L_f}(E)][1+iZ_{L_f}(E)]^{-1}v^{-1/2}\ . \tag{A15}$$

[1]E. van Beveren, C. Dullemond, and T. A. Rijken, Nijmegen Report No. THEF-NYM-79.11 (unpublished).

[2]E. van Beveren, C. Dullemond, and G. Rupp, Phys. Rev. D 21, 772 (1980).

[3]N. M. Budnev, V. M. Budnev, and V. V. Serebryakov, Phys. Lett. 70B, 365 (1977); D. Aston *et al.*, *ibid.* 92B, 211 (1980).

[4]D. Aston *et al.*, Phys. Lett. 92B, 215 (1980).

[5]F. Mané *et al.*, Phys. Lett. 99B, 261 (1981).

[6]D. Aston *et al.*, Phys. Lett. 92B, 219 (1980).

[7]A. Chodos, R. L. Jaffe, K. Johnson, C. B. Thorn, and V. F. Weisskopf, Phys. Rev. D 9, 3471 (1974); T. A. DeGrand, R. L. Jaffe, K. Johnson, and J. J. Kiskis, *ibid.* 12, 2060 (1975).

[8]N. Isgur and G. Karl, Phys. Lett. 72B, 109 (1977); Phys. Rev. D 18, 4187 (1978); Phys. Lett. 74B, 353 (1978); Phys. Rev. D 19, 2653 (1979); 20, 1191 (1979).

[9]For references to the literature see, e.g., A. Martin, Phys. Lett. 93B, 338 (1980).

[10]E. Eichten, K. Gottfried, K. D. Lane, T. Kinoshita, and T.-M. Yan, Phys. Rev. D 17, 3090 (1978); 21, 313(E) (1980); 21, 203 (1980).

[11]C. Dullemond and E. van Beveren, Ann. Phys. (N.Y.) 105, 318 (1977).

[12]For references to the literature see, e.g., J. J. de Swart and M. M. Nagels, Forsch. Phys. 28, 215 (1978).

[13]L. Micu, Nucl. Phys. B10, 521 (1969).

[14]R. Carlitz and M. Kislinger, Phys. Rev. D 2, 336 (1970).

[15]A. Le Yaouanc, L. Oliver, O. Pène, and J.-C. Raynal, Phys. Rev. D 8, 2223 (1973).

[16]M. Chaichain and R. Kögerler, Ann. Phys. (N.Y.) 124, 61 (1980).

[17]H. B. Nielsen and A. Patkós, Nucl. Phys. B195, 137 (1982).

[18]Particle Data Group, Rev. Mod. Phys. 52, S1 (1980).

[19]G. Höhler, F. Kaiser, R. Koch, and E. Pietarinen, *Handbook of Pion-Nucleon Scattering,* No. 12-1 of

Physics Data (Fachsinformationzentrum, Karlsruhe, 1979).

[20]R. Blankenbecler and R. Sugar, Phys. Rev. 142, 1051 (1966); A. A. Logunov and A. N. Tavkhelidze, Nuovo Cimento 29, 380 (1963).

[21]M. H. Partovi and E. L. Lomon, Phys. Rev. D 2, 1999 (1970).

[22]P. Mulders, Nijmegen Report No. THEF-NYM-81.6, 1981 (unpublished).

[23]E. H. Thorndike, Report No. UR-758, University of Rochester (unpublished).

[24]A. De Rújula, H. Georgi, and S. L. Glashow, Phys. Rev. D 12, 147 (1975).

[25]E. Paul, in *Proceedings of the International Symposium on Lepton and Photon Interactions at High Energies, Bonn,* edited by W. Pfeil (Universität Bonn, Bonn, 1981), p. 301.

[26]In *Higher Transcendental Functions* (Bateman Manuscript Project), edited by A. Erdélyi, W. Magnus, F. Oberhettinger, and F. G. Tricomi (McGraw-Hill, New York, 1953), Vol. 1.